Suppressing vanadium dissolution of V_2O_5 via in situ polyethylene glycol intercalation towards ultralong lifetime room/low-temperature zinc-ion batteries

Chunfa Lin,[a] Fenqiang Qi,[b] Huilong Dong,[a] Xiao Li,[a] Chunping Shen,[c] Edison Huixiang Ang,[d] Yuqiang Han,[a]* Hongbo Geng,[a]* Cheng Chao Li[e]*

[a]School of Materials Engineering, Changshu Institute of Technology, Changshu, Jiangsu, 215500, China

[b]College of Chemistry, Chemical Engineering and Materials Science, Soochow University, Suzhou 215123, China

[c]Jiangsu Tenpower Lithium Co., Ltd., Zhangjiagang, Jiangsu, China

[d]Natural Sciences and Science Education, National Institute of Education, Nanyang Technological University, Singapore, Singapore

[e]School of Chemical Engineering and Light Industry, Guangdong University of Technology, Guangzhou 510006, China

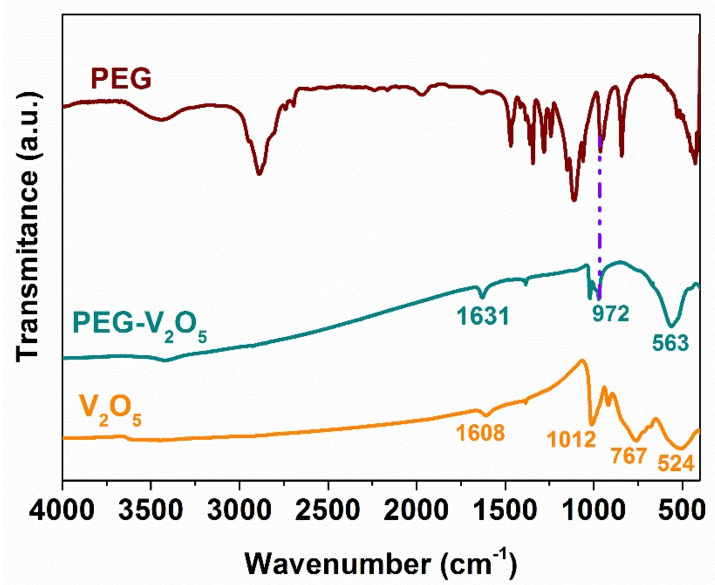

Figure S1. FTIR spectra of PEG, PEG-V_2O_5 and raw V_2O_5.

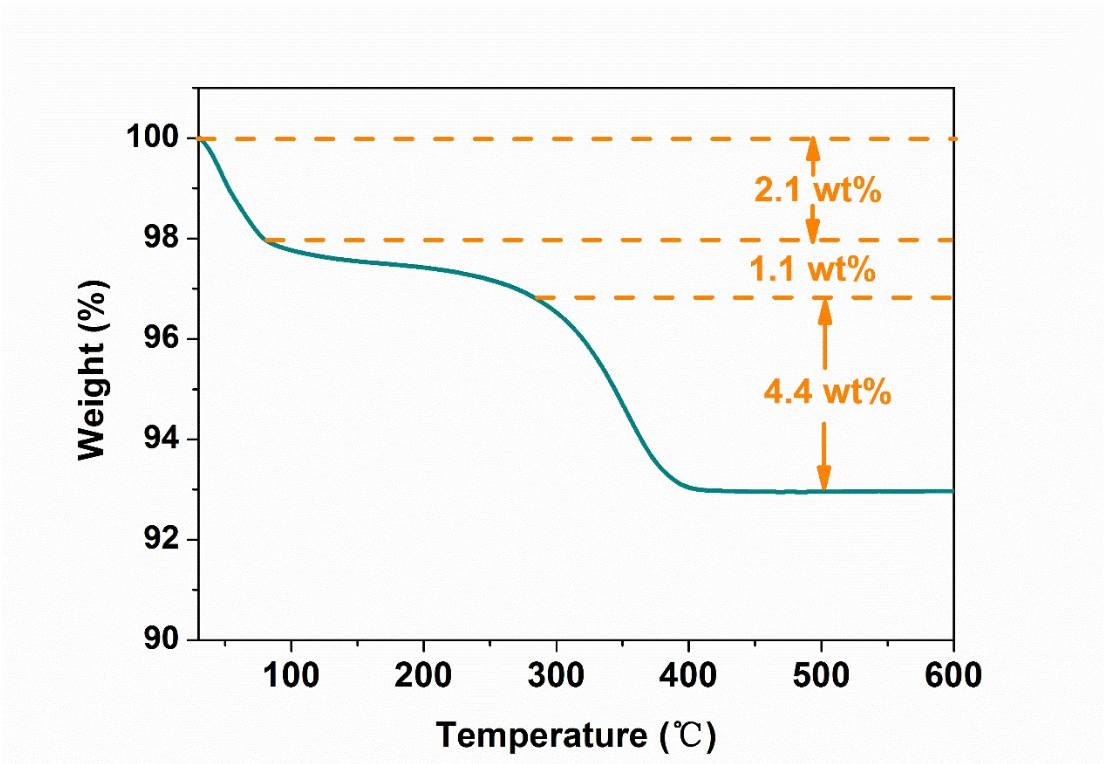

Figure S2. The TG curves of PEG-V_2O_5.

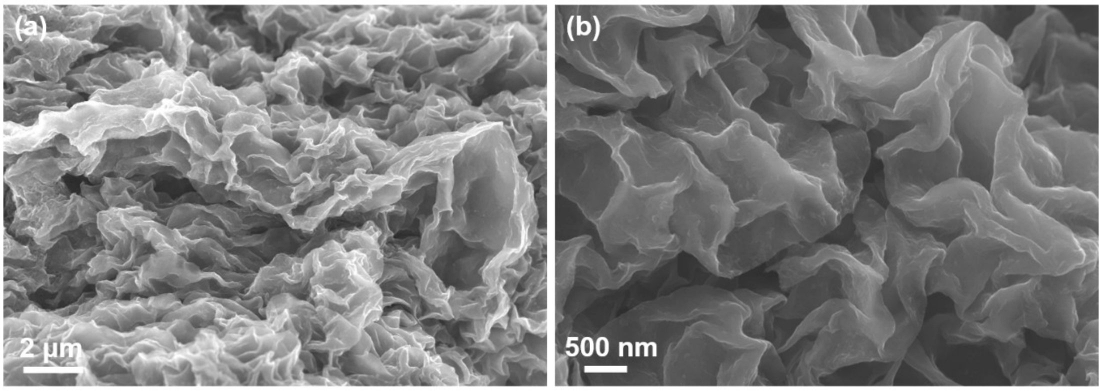

Figure S3. (a, b) SEM images of HVO.

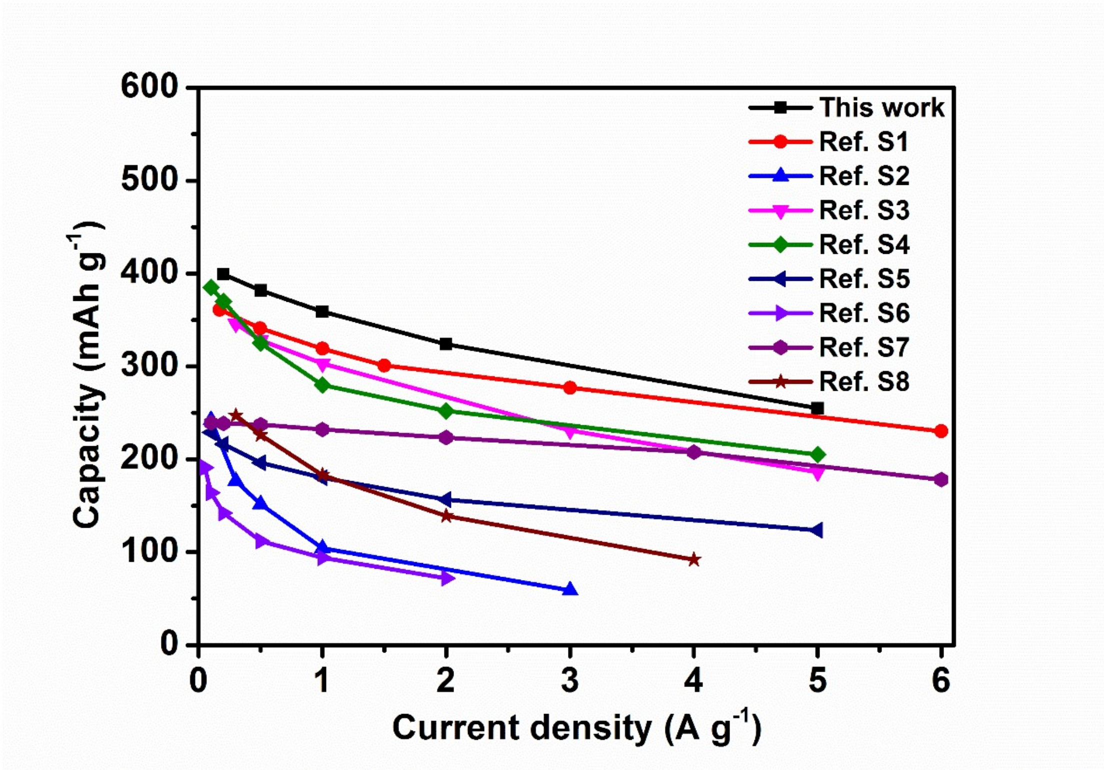

Figure S4. Comparison of the rate capability of the PEG-V_2O_5 with other previously reported ZIBs cathodes.

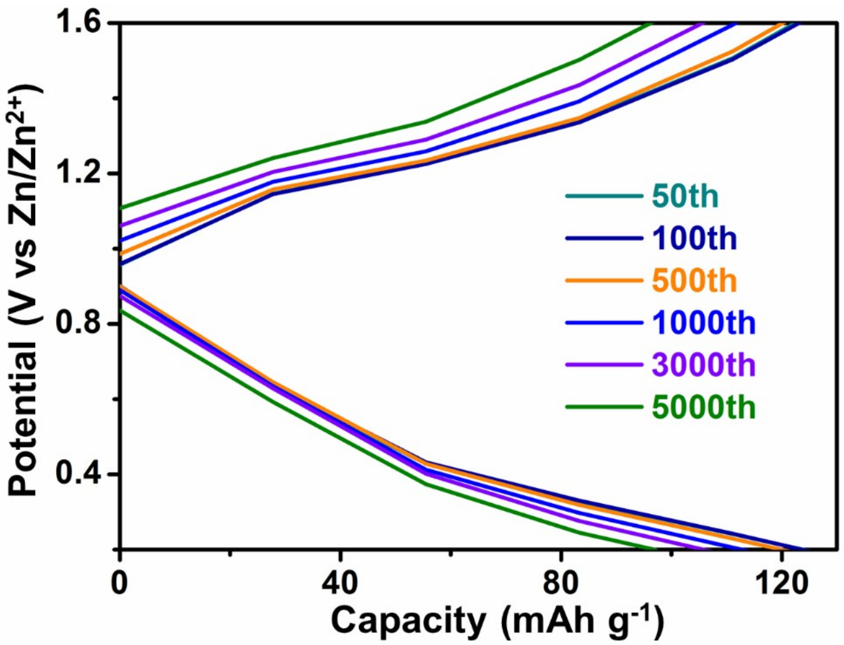

Figure S5. Galvanostatic charge-discharge profiles during different cycling numbers at 10.0 A g^{-1}.

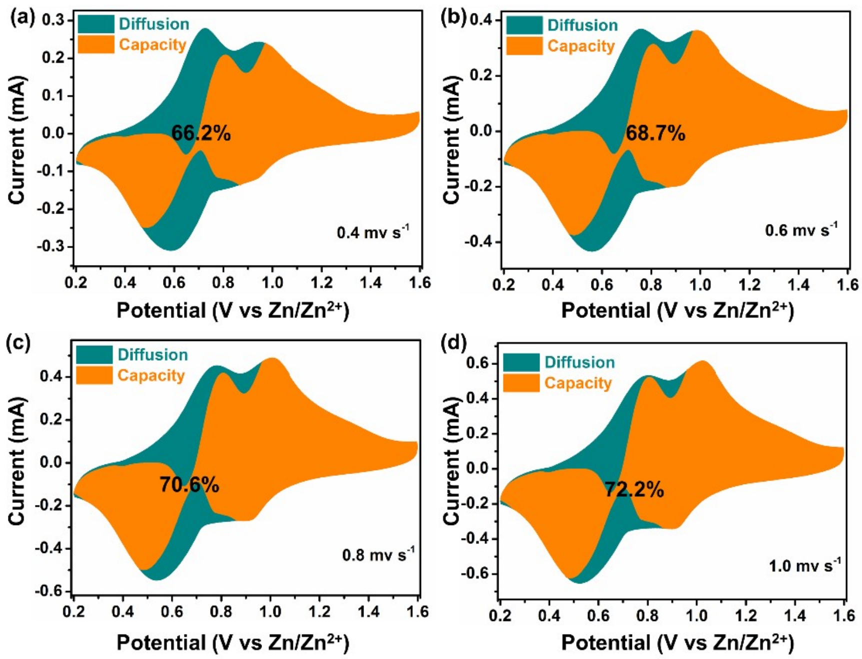

Figure S6. Separation of the capacitive and diffusion-controlled current contribution at different scan rates.

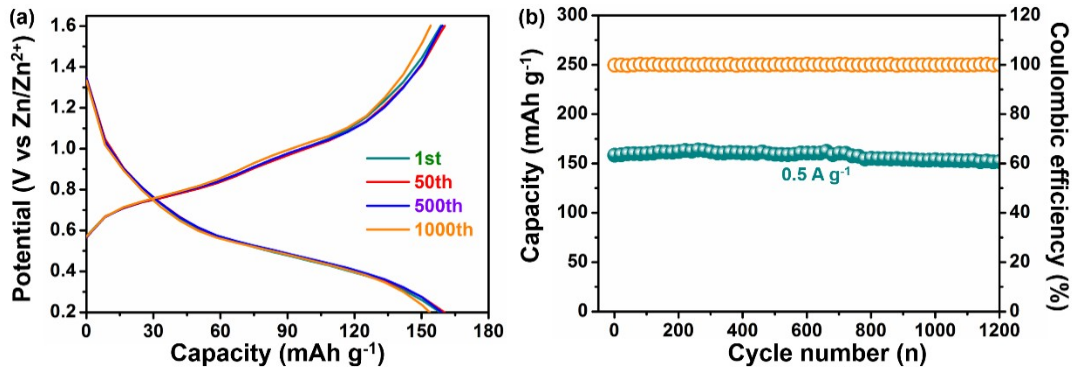

Figure S7. Zinc-ion storage performance of PEG-V_2O_5 electrode at a low temperature of -10 ^oC: (a) The charge-discharge curves and (b) cycling performance at 0.5 $A\cdot g^{-1}$.

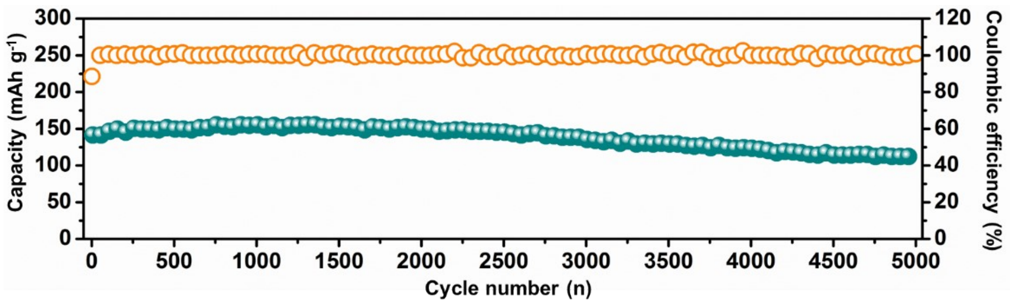

Figure S8. Long cycling performance of PEG-V_2O_5 electrode at a low temperature of -10 ^oC at 2.0 A g^{-1}.

Table S1. Comparison of the diffusion coefficient ($D_{Zn^{2+}}$)with other reported cathode materials.

Cathode Materials	$D_{Zn^{2+}}$ (cm^2 s^{-1})	Ref.
PEG-V_2O_5	10^{-9} ~ 10^{-11}	This work
$Mn_{0.15}V_2O_5$•nH_2O	10^{-10} ~ 10^{-12}	[9]
α-MnO_2	10^{-12} ~ 10^{-17}	[2]
$LiFePO_4$	10^{-15} ~ 10^{-19}	[10]
MnO_2 nanospheres	10^{-12} ~ 10^{-15}	[11]
δ-MnO_2	10^{-12} ~ 10^{-15}	[12]
PANI-VOH	10^{-13} ~10^{-16}	[3]
$Al_{0.2}V_2O_5$	10^{-12} ~ 10^{-13}	[13]

References:

S1. V. Soundharrajan, B. Sambandam, S. Kim, M.H. Alfaruqi, D.Y. Putro, J. Jo, S. Kim, V. Mathew, Y.K. Sun and J. Kim, *Nano Lett.*, 2018, **18**, 2402-2410.

S2. B. Wu, G. Zhang, M. Yan, T. Xiong, P. He, L. He, X. Xu and L. Mai, *Small*, 2018, **14**, 1703850.

S3. M. Wang, J. Zhang, L. Zhang, J. Li, W. Wang, Z. Yang, L. Zhang, Y. Wang, J. Chen, Y. Huang, D. Mitlin and X. Li, *ACS Appl. Mater. Interfaces*, 2020, **12**, 31564-31574.

S4. F. Wan, S. Huang, H. Cao and Z. Niu, *ACS Nano*, 2020, **14**, 6752-6760.

S5. T. Wei, Q. Li, G. Yang, C. Wang, *J. Mater. Chem. A*, 2018, **6**, 20402-20410.

S6. Y. Cai, F. Liu, Z. Luo, G. Fang, J. Zhou, A. Pan and S. Liang, *Energy Storage Mater.*, 2018, **13**, 168-174.

S7. B. Sambandam, V. Soundharrajan, S. Kim, M.H. Alfaruqi, J. Jo, S. Kim, V.

Mathew, Y.K. Sun and J. Kim, *J. Mater. Chem. A*, 2018, **6**, 15530-15539.

S8. B. Tang, G. Fang, J. Zhou, L. Wang, Y. Lei, C. Wang, T. Lin, Y. Tang and S. Liang, *Nano Energy*, 2018, **51**, 579-587.

S9. H. Geng, M. Cheng, B. Wang, Y. Yang, Y. Zhang and C.C. Li, *Adv. Funct. Mater.*, 2019, **30**, 1907684.

S10. K. Tang, X. Yu, J. Sun, H. Li and X. Huang, *Electrochim. Acta*, 2011, **56**, 4869-4875.

S11. J. Wang, J.-G. Wang, H. Liu, C. Wei and F. Kang, *J. Mater. Chem. A*, 2019, **7** 13727-13735.

S12. C. Guo, H. Liu, J. Li, Z. Hou, J. Liang, J. Zhou, Y. Zhu and Y. Qian, *Electrochim. Acta*, 2019, **304**, 370-377.

S13. Q. Pang, W. He, X. Yu, S. Yang, H. Zhao, Y. Fu, M. Xing, Y. Tian, X. Luo and Y. Wei, *Appl. Surf. Sci.*, 2021, **538**, 148043.